26. Kemp BJ, Prato FS, Nicholson RL, Reese L. Transmission computed tomography imaging of the head with a SPECT system and a collimated line source. *J Nucl Med* 1995;36:328–335.
27. Chang W, Loncaric S, Huang G, Sanpitak P. Asymmetric fan transmission CT on SPECT systems. *Phys Med Biol* 1995;40:913–928.
28. Hawman EG, Ficaro EP, Hamill JJ, Schwaiger M. Fanbeam collimation with off center focus for simultaneous emission/transmission SPECT in multicamera SPECT systems [Abstract]. *J Nucl Med* 1994;35:92.
29. Tsui BMW, Lalush DS, Lewis DP, et al. High-resolution brain SPECT imaging using half fanbeam collimators with a right-angle, dual-camera SPECT system [Abstract]. *J Nucl Med* 1997;38:32P.
30. Tomiguchi S, Kojima A, Oyama Y, et al. Development of asymmetric fanbeam transmission CT on two-head SPECT system [Abstract]. *J Nucl Med* 1997;38:212P.
31. Gilland DR, Jaszczak RJ, Wang H, Coleman RE. Transmission data acquisition with a large-field-of-view dual-head SPECT system [Abstract]. *J Nucl Med* 1997;38:220P.
32. Gilland DR, Wang H, Coleman RE, Jaszczak RJ. Long focal length, asymmetric fanbeam collimation for transmission acquisition with a triple camera SPECT system. *IEEE Trans Nucl Sci* 1997;44:1191–1196.
33. Beekman FJ, Kamphuis C, van Rijk PP. Scanning point sources combined with two half-fanbeam collimators for simultaneous emission and transmission measurements in SPECT [Abstract] *J Nucl Med* 1997;38:216P.
34. Heller EN, DeMan P, Liu YH, et al. Extracardiac activity complicates quantitative cardiac SPECT imaging using a simultaneous transmission-emission approach. *J Nucl Med* 1997;38:1882–1890.
35. Manglos SH, Bassano DA, Duxbury C, Capone R. Attenuation maps for SPECT determined using cone beam transmission computed tomography. *IEEE Trans Nucl Sci* 1990;37:600–607.
36. Lange K, Fessler JA. Globally convergent algorithms for maximum a posteriori transmission tomography. *IEEE Trans Im Proc* 1995;4:1430–1438.
37. Zeng GL, Hsieh Y, Gullberg GT. A rotating and warping projector-backprojector pair for fanbeam and cone-beam iterative algorithms. *IEEE Trans Nucl Sci* 1994;41:2807–2811.
38. Lange K, Carson REM. Reconstruction algorithms for emission and transmission tomography. *J Comput Assist Tomogr* 1984;8:306–316.
39. Tsui BMW, Zhao XD, Gregouri GK, et al. Quantitative cardiac SPECT reconstruction with reduced image degradation due to patient anatomy. *IEEE Trans Nucl Sci* 1993;41:2838–2844.
40. Jaszczak RJ, Gilland DR, McCormick JW, Scarphone C, Coleman RE. The effect of truncation reduction in fan beam transmission for attenuation correction in cardiac SPECT. *IEEE Trans Nucl Sci* 1996;43:2255–2262.
41. Tung CH, Gullberg GT, Zeng GL, Christian PE, Datz FL, Morgan HT. Nonuniform attenuation correction using simultaneous transmission and emission converging tomography. *IEEE Trans Nucl Sci* 1992;38:1134–1143.
42. King MA, Luo D, Dahlberg S, Penney B, Morgan H. Transmission imaging of large attenuators using a slant hole collimator on a three-head SPECT system. *Med Phys* 1996;23:263–272.
43. Beekman FJ, Kamphuis C. Effects of truncation of transmission projections on cardiac SPECT images acquired by a right-angle dual-camera with half-fanbeam collimators *Conference record of 1997 IEEE nuclear science symposium and medical imaging conference.* Albuquerque, NM: IEEE *Trans Nucl Sci* 1998;45:1174–1178.
44. Luo D, King MA, Morgan HT, et al. Investigations into possible causes of hot inferior wall artifacts in attenuation-corrected cardiac perfusion images. *IEEE Trans Nucl Sci* 1997;44:1146–1153.
45. Floyd CE, Jaszczak RJ, Harris CC, Coleman RE. Energy and spatial distribution of multiple order Compton scatter in SPECT; a Monte Carlo investigation. *Phys Med Biol* 1984;29:1217–1230.
46. Beekman FJ, Viergever MA. Fast SPECT simulation including object shape dependent scatter. *IEEE Trans Med Imaging* 1995;14:271–282.
47. Frey EC, Tsui BMW. A new method for modeling the spatially variant object dependent scatter response function in SPECT. *1996 IEEE nuclear science symposium conference record.* Anaheim, CA: IEEE; November 1996:1082–1086.
48. Kadrmas DJ, Jaszczak RJ, McCormick JW, Coleman RE, Lim CB. Truncation artifact reduction in transmission CT for improved SPECT attenuation compensation. *Phys Med Biol* 1995;40:1085–1104.
49. Zeng GL, Gullberg GT. An SVD study of truncated transmission data in SPECT. *IEEE Trans Nucl Sci* 1997;44:107–111.

Imaging of Adenoviral-Directed Herpes Simplex Virus Type 1 Thymidine Kinase Reporter Gene Expression in Mice with Radiolabeled Ganciclovir

Sanjiv S. Gambhir, Jorge R. Barrio, Lily Wu, Meera Iyer, Mohammad Namavari, Nagichettiar Satyamurthy, Eileen Bauer, Capella Parrish, Duncan C. MacLaren, Ali R. Borghei, Leeta A. Green, Susan Sharfstein, Arnold J. Berk, Simon R. Cherry, Michael E. Phelps and Harvey R. Herschman

Crump Institute for Biological Imaging; UCLA/DOE Laboratory of Structural Biology and Molecular Medicine; Department of Molecular and Medical Pharmacology, Division of Nuclear Medicine; Molecular Biology Institute; Department of Biomathematics; and UCLA-Jonsson Comprehensive Cancer Center, UCLA School of Medicine, Los Angeles, California

We are developing procedures to repeatedly and noninvasively image the expression of transplanted reporter genes in living animals and in patients, using PET. We have investigated the use of the Herpes Simplex Virus type 1 thymidine kinase gene (HSV1-tk) as a reporter gene and [8-^{14}C]-ganciclovir as a reporter probe. HSV1-tk, when expressed, leads to phosphorylation of [8-^{14}C]-ganciclovir. As a result, specific accumulation of phosphorylated [8-^{14}C]-ganciclovir should occur almost exclusively in tissues expressing the HSV1-tk gene. **Methods:** An adenoviral vector was constructed carrying the HSV1-tk gene along with a control vector. C6 rat glioma cells were infected with either viral vector and uptake of [8-^{3}H]-ganciclovir was determined. In addition, 12 mice were injected with varying levels of either viral vector. Adenovirus administration in mice leads primarily to liver infection. Forty-eight hours later the mice were injected with [8-^{14}C]-ganciclovir, and 1 hr later the mice were sacrificed and biodistribution studies performed. Digital whole-body autoradiography also was performed on separate animals. HSV1-tk expression was assayed, using both normalized HSV1-tk mRNA levels and relative HSV1-TK enzyme levels, in both the cell culture and murine studies. **Results:** Cell culture, murine tissue biodistribution and murine in vivo digital whole-body autoradiography all demonstrate the feasibility of HSV1-tk as a reporter gene and [8-^{14}C]-ganciclovir as an imaging reporter probe. A good correlation (r^2 = 0.86) between the [8-^{14}C]-ganciclovir percent injected dose per gram tissue from HSV1-tk positive tissues and HSV1-TK enzyme levels in vivo was found. An initial study in mice with [8-^{18}F]-fluoroganciclovir and microPET imaging supports further investigation of [8-^{18}F]-fluoroganciclovir as a PET reporter probe for imaging HSV1-tk gene expression. **Conclusion:** These results demonstrate the feasibility of using [8-^{14}C]-ganciclovir as a reporter probe for the HSV1-tk reporter gene, using an in vivo adenoviral mediated gene delivery system in a murine model. The results form the foundation for further investigation of [8-^{18}F]-fluoroganciclovir for noninvasive and repeated imaging of gene expression with PET.

Key Words: reporter gene; imaging; PET; thymidine kinase; gene expression

J Nucl Med 1998; 39:2003–2011

Received Mar. 2, 1998; revision accepted May 6, 1998.

For correspondence or reprints contact: Sanjiv S. Gambhir, UCLA School of Medicine, 700 Westwood Plaza, A-222B CIBI, Los Angeles, CA 90095-1770.

Current methods to image the expression of reporter genes in experimental animals and humans require the use of tissue, obtained either from biopsy or after death. Alternatives for noninvasively and repeatedly imaging gene expression in animals are currently limited. Animals transparent to visible light (e.g., nematodes) can be imaged using the green fluorescent protein (*1*) as a reporter, and some small animals (e.g., mice) can be imaged using the luciferase reporter gene (*2*). Both of these methods rely on a simple video camera for imaging. However, these techniques are not generalizable to humans, and do not give access to all tissues throughout the body. Development of procedures to repeatedly and noninvasively monitor reporter gene expression in mammals would permit new experimental approaches to study transgenic animals, adoptive cell therapy, tracking of infections (e.g., viral), and human gene therapy. Use of reporter genes encoding proteins able either to metabolize positron-labeled "PET reporter substrates" to trapped products or to bind positron-labeled "PET reporter ligands" should provide novel assays to image reporter gene expression in living animals.

The herpes simplex virus Type 1 thymidine kinase gene (HSV1-tk) is an attractive candidate for use in noninvasive reporter gene imaging by PET, since several substrates, including but not limited to acyclovir (acycloguanosine) (ACV), ganciclovir (GCV), 5-iododeoxyuridine, 2′-fluoro-2′ deoxy-1-5-iodo-1-β-D-arabinofuranosyl-5-iodo-uracil (FIAU), can be phosphorylated by HSV1-TK (*3–5*). *Note that HSV1-tk refers to the gene and HSV1-TK refers to the enzyme.* Tjuvajev et al. (*6*) demonstrated the utility of HSV1-tk as a "marker gene" and [2-^{14}C]-FIAU as "marker substrate" for autoradiographic imaging of tissue sections from transplanted brain tumors expressing HSV1-tk. More recently, the same authors used [^{131}I]-FIAU to image HSV1-tk expressed in tumors in vivo, by SPECT (*7*), and have presented preliminary findings in abstract form with [^{124}I]-FIAU and PET in athymic rats (*8*). We have been developing a similar approach to image HSV1-tk reporter gene expression, using acycloguanosine derivatives (i.e., ACV, GCV) (*9*). Haberkorn et al. (*10*) also have recently described the use of [8-^{3}H]-ganciclovir in HSV1-tk positive cell lines to detect HSV1-tk gene expression in cultured cells, but have not reported any results in vivo. The cytosine deaminase gene and cytosine also have been studied as a reporter gene/reporter probe system. However, this system has not worked well due to a lack of sufficient accumulation of [^{3}H]−5-fluorocytosine in cytosine deaminase expressing cells (*11*). We also have investigated an alternate reporter gene/reporter probe system, using the dopamine D2-receptor gene as a reporter gene and 3-([2′-^{18}F]-fluoroethyl)spiperone as a reporter probe for PET imaging in vivo, with good preliminary results in tumors expressing the D2 receptors that have been implanted in nude mice (*12*).

ACV and GCV have been extensively studied as pharmaceuticals for treating herpes viral infections (*13,14*). After transport into cells through nucleobase and/or nucleoside transporters (*15,16*), ACV and GCV are phosphorylated to the monophosphate form by HSV1-TK. After further phosphorylation by cellular kinases, ACV/GCV-triphosphates are incorporated into DNA, where these acyclic guanosine analogs block viral DNA chain elongation. Two factors make acycloguanosine derivatives attractive as drugs as well as biological probes: First, ACV and GCV undergo only minimal metabolism in vivo (*13,14*). Second, ACV and GCV are minimally phosphorylated by endogenous mammalian cytoplasmic and mitochondrial thymidine kinases (*17,18*). In contrast to thymidine, or closely related deoxyribosides of 5-iodouridine derivatives (e.g., FIAU), acycloguanosine analogues show very high specificity for the viral enzyme (*19,20*).

Because of the extensive knowledge of murine genetics and the ability to manipulate the murine genome by both transgenic and homologous recombination procedures, the mouse has become the animal of choice in most contemporary in vivo studies of gene expression, development and function of the immune system, tumor cell growth and suppression, and preclinical gene therapy models. We anticipate that the ability to repeatedly and noninvasively monitor gene expression in vivo will be of value in all these areas.

For PET studies, replacement of the 8-hydrogen in acycloguanosine by fluorine would be expected to cause only minimal steric perturbations in HSV1-TK binding, since fluorine has a van der Waals radius (1.35 Å) similar to that of hydrogen (1.20 Å) (*19*). Moreover, the increased stability of the C-F bond relative to the C-H bond might also result in increased chemical and in vivo metabolic stability. We have investigated this strategy (*20–22*) with [8-^{18}F]-fluoroganciclovir ([8-^{18}F]-FGCV) and [8-^{18}F]-fluoroacyclovir ([8-^{18}F]-FACV). Monclus et al. (*23*) and Allaudin et al. (*24*) recently have reported the labeling of ganciclovir in the side-chain with ^{18}F, which resulted in an enantiomeric mixture of products. Bading et al. (*25*) have used an identically labeled ganciclovir in primates and preliminary reported in abstract form (one animal) the biodistribution of the probe.

In this study we investigate [side-chain-2-^{3}H]-acyclovir and [8-^{3}H]-ganciclovir as probes to monitor HSV1-tk gene expression in cell culture. We then use a murine model and a viral gene delivery system to image HSV1-tk reporter gene expression in vivo. When mice are injected intravenously with recombinant adenoviruses, reporter gene expression is overwhelmingly directed to the liver (*26*). We explore the biodistribution of [8-^{14}C]-ganciclovir in vivo, in a murine model, to investigate the utility of this compound as a reporter probe. We directly correlate the level of accumulation of [8-^{14}C]-GCV in HSV1-tk transduced tissues with reporter gene expression, as measured by normalized HSV1-tk mRNA levels and by HSV1-TK enzyme levels, using an adenoviral delivery mechanism to direct HSV1-tk primarily to the mouse liver. We also use digital whole-body autoradiography (DWBA) imaging, to demonstrate the ability of [8-^{14}C]-GCV to image HSV1-tk expression in vivo. Finally, we preliminarily explore the feasibility of imaging gene expression with [8-^{18}F]-FGCV and microPET imaging (*27*) while using the same murine model.

MATERIALS AND METHODS

Radiolabeled Compounds

[8-^{14}C]-acyclovir ([8-^{14}C]-ACV) (56 mCi/mmol; mol wt = 225.2), [8-^{14}C]-ganciclovir ([8-^{14}C]-GCV) (specific activity 55 mCi/mmol; mol wt = 255.2), [2-^{14}C]-thymidine ([2-^{14}C]-THD) (specific activity 56 mCi/mmol; mol wt = 242.2) were obtained from Moravek Biochemicals, Inc. (Brea, CA). Reported purity was 99.9%, 99.8%, 99.7% for [8-^{14}C]-ACV, [8-^{14}C]-GCV, [2-^{14}C]-THD, respectively. [side-chain-2-^{3}H]-acyclovir ([side-chain−2-^{3}H]-ACV) (18.3 Ci/mmol; mol wt = 225.2), and [8-^{3}H]-ganciclovir ([8-^{3}H]-GCV) (13.1 Ci/mmol; mol wt = 255.2) also were obtained from Moravek Biochemicals, Inc. with a reported purity greater than 98%. Radiochemical purities were determined before use for all radiochemicals purchased using high-performance liquid chromatography (HPLC), and were found to be greater than 97%.

Radioactivity Counting

All ^{3}H counting was performed using a Beckman LS-9000 liquid scintillation counter with Biosafe II (Research Products International, Costa Mesa, CA) scintillation fluid. For ^{14}C tissue counting, small samples of the tissue (0.009–0.0005 g) were dissolved with hyamine and heated at 50°C for ~12 hr before counting with cytoscint (ICN, Inc., Costa Mesa, CA) scintillation fluid. Corrections for background activity and efficiency (96.1% for ^{14}C and 51.4% for ^{3}H) based on calibrated standards (Beckman, Inc.) also were performed to obtain disintegrations per minute (dpm). Tritium counts also were corrected for quenching effects. Corrections for the efficiency of tissue sample counting were performed by sending random tissue samples (PTRL, Inc., Richmond, CA) for counting by a combustion method (*28*).

Preparation of an Adenovirus Vector Expressing HSV1-tk

A 1.9-kb *Eco*R I to *Sac* II fragment containing the herpes HSV1-tk gene open reading frame, as provided by William Clark (UCLA, Los Angeles, CA), was cloned into pBS II SK+ (Stratagene, Inc., La Jolla, CA), to construct pBS-HSV1-tk. The Sst II site of pBS-HSV1-tk was converted to an *Xba* I site by ligation to the two oligonucleotides 5′-CCTCTAGAGG-TACGGC-3′ and 5′-CGTACCTCTAGAGGGC-3′, generating pBS-HSV1-tkX. The *Eco*R I to *Xba* I fragment, containing HSV1-tk, was inserted between the cytomegalovirus (CMV) immediate-early promoter and the SV40 splice and polyA site of pACCMVpLpASR (*29*). AdCMV-HSV1-tk recombinant virus was constructed by co-transfection of 293 cells with pACCMVpLpASR-HSV1-tk and d1309 viral DNA (*30*) that had been cut with *Xba* I and *Cla* I. AdCMV-HSV1-tk was plaque purified on 293 cells three times and grown into a high titer stock of 1×10^{10} plaque forming units (pfu)/ml, as assayed by plaque formation on 293 cells. The control virus, Ad5-dl434, is an E1 deletion mutant with viral sequences between 2.6 and 8.7 map units deleted (*31*).

Cell Lines and Culture Conditions

C6 rat glioma cells obtained from the American Type Culture Collection were grown as monolayers in t75 flasks in DME supplemented with 5% FBS, 1% penicillin-streptomycin, and 1% L-glutamine. Twenty-four hours after plating, either 1×10^{9} pfu/ml of AdCMV-HSV1-tk virus (to produce C6 tk+cells) or 1×10^{9} pful/ml of control virus (to produce C6 tk−cells) were added to separate flasks. Exposure to the adenovirus was over a 27-hr period, followed by replating and growth over an additional 22 hr in 12-well plates (for tracer uptake studies), or 100-mm dishes (for determination of relative HSV1-tk enzyme levels and mRNA levels).

Cell Culture Uptake Studies

C6tk+ and C6tk- cells were incubated with [8-^{3}H]-GCV at concentrations of 0.82 μCi/ml (1.44×10^{-5} mg/ml) in culture medium. The wells were incubated at 37°C for 15, 30, 60, 120 and 240 min. At the end of each incubation period, the radioactive medium was removed and radioactivity was determined. The wells were washed with cold phosphate-buffered saline, the cells were harvested using a cell scraper, and the cell-associated radioactivity also was determined. Triplicate samples were performed at each time point. The same wells also were used for determining total protein content for each infected population (*32*). Data are expressed as the net accumulation of probe in [dpm cells/(dpm of medium at start of exposure)/μg protein] ± s.e. Uptake studies also were performed while using [side-chain−2-^{3}H]-ACV.

HSV1-TK Enzyme Assay

This assay was used to determine the relative levels of HSV1-TK enzyme activity in both cultured cells and mouse tissue extracts. The assay is based on incubating cell or tissue extracts with [8-^{3}H]-GCV, and then [8-^{3}H]-GCV is separated from phosphorylated [8-^{3}H]-GCV, as previously described (*33*). For the cell culture studies, $\sim 2 \times 10^{6}$ cells were trypsinized and dissolved in 40 μl PBS. For the murine studies, ~0.1–0.4 g organ was dissolved in 3.0 ml PBS. All samples were frozen at −80°C for ~24 hr before being assayed. Sample protein determinations also were made (*32*). Both liver and muscle samples were assayed. All results were converted to dpm/μg protein/min. Linearity of the assay with respect to enzyme concentration and reaction time also was checked. The reproducibility of this assay was within ± 15% s.d. based on repeated assaying.

Northern Blot Analysis

For cell culture studies, total RNA was extracted from cell lysates. For mouse studies, the liver was rapidly dissected, weighed and homogenized in a guanidium thiocyanate solution containing β-mercaptoethanol. The total RNA then was extracted using phenol as described previously (*34*). Total RNA was subjected to electrophoresis under denaturing conditions on a 1.2% agarose-formaldehyde gel (10 μg RNA/lane). Hybridization was performed with [^{32}P] (random primed) labeled HSV1-tk probe (derived from HSV-TK cDNA) overnight at 42°C. Hybridizations done with a GAPDH specific [^{32}P] labeled DNA probe, were used to normalize the samples for total mRNA content. The relative photo-stimulated luminescence (PSL)/mm^2 values for the HSV1-tk and GAPDH bands were measured (using a 5000 Phosphorimager (Fuji Photo Film Co., Ltd., Tokyo, Japan) and digital plates) to obtain the normalized HSV1-tk mRNA levels by calculating the ratio of relative intensities of HSV1-tk to that of GAPDH [(PSL/mm^2 HSV1-tk Band 1 + PSL/mm^2 HSV1-tk Band 2) ÷ PSL/mm^2 GAPDH].

Murine Biodistribution Studies

Animal care and euthanasia were performed using criteria approved by the UCLA Animal Research Committee. Adult 10–12-wk-old Swiss webster mice (25–35 g) were injected through the tail vein with 1×10^{9} pfu of either AdCMV-HSV1-tk virus or E1-deleted Ad5-d1434 control virus. Three mice were used for each category. Forty-eight (±1) hours later the animals received a tail vein injection of [8-^{14}C]-GCV (2.5 μCi in 0.1–0.2 ml) followed by a saline flush of 0.1 ml. The probe was allowed to distribute for 60 ± 4 min before sacrificing the mouse. Radioactivity determinations were normalized by the weight of the tissue and amount of radioactivity injected, to obtain percent injected dose per gram of tissue (%ID/g). To determine the effects of varying levels of active HSV1-TK enzyme on [8-^{14}C]-GCV uptake, increasing amounts of AdCMV-HSV1-tk (0.50×10^{9} and 0.75×10^{9}) were injected into a total of 6 mice (3 mice for each pfu level) and the experiments for biodistribution repeated. Small samples of liver (0.1–0.4 g each) also were used for determining normalized HSV1-tk mRNA levels and enzyme activity levels in 8 of the 12 mice studied. Muscle samples served as control tissue for each mouse. In 4 additional mice injected with control virus, the biodistribution studies were performed by sacrificing the animal at 5, 20, 40 and 120 min after injection of [8-^{14}C]-GCV.

Autoradiography

The viral administration and ganciclovir exposure procedure described in the biodistribution studies above was repeated,

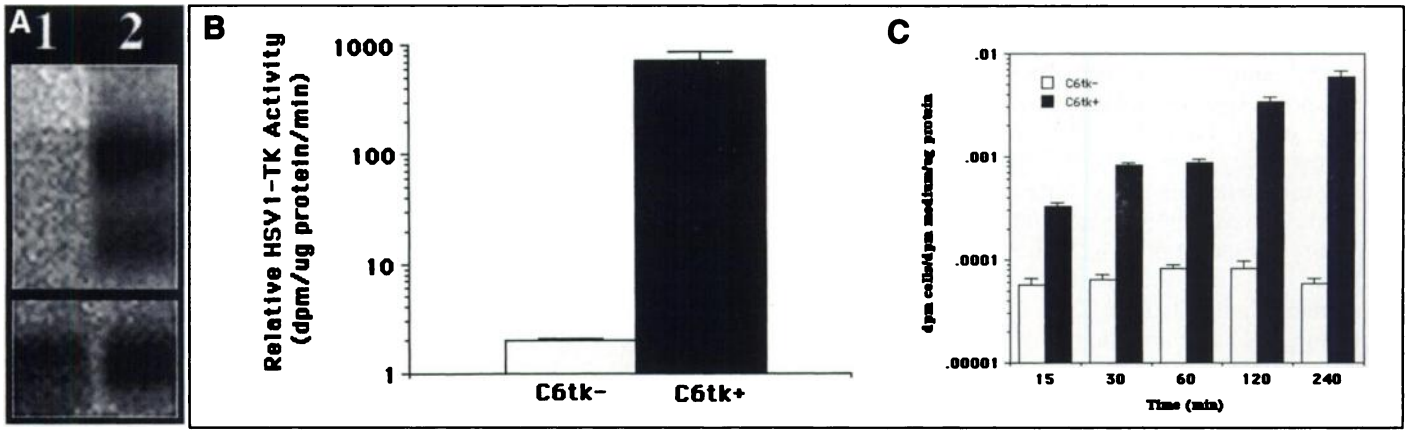

FIGURE 1. (A) Northern blot of RNA extracted from C6 cells infected with control virus (C6tk-) and AdCMV-HSV1-tk virus (C6tk+) in lanes 1 and 2, respectively. Top two bands obtained in lane 2 are from presence of HSV1-tk transcripts (upper panel) and bottom band in both lanes are from GAPDH (lower panel). (B) Relative HSV1-TK enzyme activity (*log scale*) from C6 cells infected with control virus (C6tk-) and AdCMV-HSV1-tk virus (C6tk+). Mean ± s.e. from triplicate determinations of relative HSV1-TK activity are shown. There is a significant difference ($p < 0.001$) between C6tk- and C6tk+ relative HSV1-TK activities. (C) [8-^{3}H]-GCV net accumulation (*log scale*) in C6tk- and C6tk+ cell lines as function of time (15, 30, 60, 120, 240 min). Shown are mean ± s.e. from triplicate samples. There is a significant difference ($p < 0.001$) between C6tk- and C6tk+ cells for all time points.

using 2 mice injected with control adenovirus and 4 mice injected with AdCMV-HSV1-tk virus (2 with 1.0×10^9 pfu, and 2 with 0.5×10^9 pfu). However, after sacrificing, each animal was frozen in liquid nitrogen in preparation for DWBA using a 45-μM slice thickness (*35*). The exposure time was 24–72 hr. All digital plates were scanned on a Fuji Bas 5000 digital autoradiographic system at 100-μM resolution. The photo-stimulated luminescence (PSL)/mm^2 in the liver was obtained using software (Mac Bas version 2.4, Fuji Photo Film Co., Ltd.) and converted to μCi/g plastic using the standard calibration curve obtained from the reference standards (*36*). Multiple regions of interest (ROI) were drawn on the images of the liver by directly superimposing the digitized photographs of the anatomical section. These values were then converted to μCi/g tissue, using a calibration curve obtained for 45-μM-thick slices, direct organ counting, and ^{14}C standards. All exposures were performed over a linear range of response for the digital plates, and verified by the linearity of the calibration curve. These values were converted to percent injected dose (%ID)/g tissue, using the known total injected dose for each mouse.

microPET Imaging

To *preliminarily* test the feasibility of imaging with [8-^{18}F]-FGCV and microPET, we performed studies with a murine model using the adenoviral vector delivery system. The [8-^{18}F]-FGCV was synthesized (specific activity of ~3–5 Ci/mmol) as previously described (*22*). Three mice were injected through the tail vein with 1.0×10^9 pfu of the control virus, and 3 mice with 1.0×10^9 pfu of AdCMV-HSV1-tk virus. Forty-eight hours later each mouse was injected through the tail vein with 150 μCi of [8-^{18}F]-FGCV. After 1 hr of probe distribution, the mice were anesthetized with Avertin (Aldrich, Milwaukee, WI), and imaged using a microPET scanner with a 2^3 mm^3 volumetric resolution (*27*). The long axis of the mouse was parallel to the long axis of the scanner, and 8 bed positions with 8 min per bed were used. No transmission scan was performed, and the images were reconstructed while using a Shepp-Logan filter with a 0.5 cutoff frequency. Mouse urine was collected at 60 min to assess the stability of [8-^{18}F]-FGCV using HPLC.

Statistical Analysis

All analyses were performed using a Student's t-test for independent samples to compare the results from two experimental groups.

RESULTS

Cell Culture Studies

We first performed a Northern blot analysis on RNA isolated from both C6tk+ and C6tk- cells. Shown in Figure 1A are the results of the Northern probed for both HSV1-tk and GAPDH mRNA. A GAPDH band is seen for both the C6tk+ and C6tk- cells. Two HSV1-tk bands (presumably representing alternately terminated transcripts) are seen for RNA extracted from the C6tk+ cells and no HSV1-tk band is present for the RNA extracted from the C6tk- cells. The ratio of HSV1-tk:GAPDH is 5.1:1 for C6tk+ and ~0 for C6tk- cells.

We next determined the relative levels of HSV1-TK enzyme in both the C6tk+ and C6tk- cells (Fig. 1B). There was a significant difference in the relative levels of HSV1-TK enzyme between the cells ($p < 0.001$). The northern blot and HSV1-TK enzyme assay results establish the successful delivery and expression of the HSV1-tk gene by the AdCMV-HSV1-tk virus into C6 cells, as well as the lack of HSV1-tk expression when using the control virus.

We next examined the ability of the C6tk+ and C6tk- cells to accumulate radioactive reporter probe. Figure 1C shows the net accumulation of [8-^{3}H]-GCV tracer as a function of time. Note the higher levels of accumulation of [8-^{3}H]-GCV in the C6tk+ cell line as compared with the HSV1-tk negative (C6tk-) cell line at 15, 30, 60, 120 and 240 min ($p < 0.001$). These results demonstrate that the net accumulation of radioactivity in the C6tk+ cells is attributable directly to the delivery and expression of the HSV1-tk gene.

The [8-^{3}H]-ACV showed significant accumulation in the C6tk+ cell line as compared to the control C6tk- cell line (1.9:1) only at relatively higher concentrations (1.2×10^{-4} mg/ml = 10 μCi/ml) and at longer incubation times of 18 hr. This would make radiolabeled forms of ACV less likely to be useful for imaging with PET (because of the relatively short half-life of positron-emitting isotopes). We therefore only pursued radiolabeled ganciclovir as a probe to develop a quantitative assay for imaging expression of the HSV1-tk reporter gene in vivo.

Murine Biodistribution Studies

We then determined whether [8-^{14}C]-GCV accumulation can be used to monitor HSV1-tk expression in vivo. Mice were injected intravenously with either a control adenovirus or an adenovirus carrying the HSV1-tk reporter gene. When adeno-

virus is injected into mice, the reporter gene expression is restricted almost completely to the liver (*26*). Two days after viral administration the mice received an intravenous injection of [8-^{14}C]-GCV and were sacrificed 1 hr later. Figure 2 shows a bar graph of the [8-^{14}C]-GCV % ID/g tissue in different tissues for both control virus and the AdCMV-HSV1-tk virus (administered at various concentrations). Each bar represents the mean ± s.e. from 3 mice. Other organs not shown (pancreas, heart, thymus, testes, stomach) all had less than 0.5% ID/g tissue. No statistically significant difference in the net accumulated activity in the liver versus muscle is observed when using the control virus ($p < 0.01$). In contrast, there is a statistically significant difference ($p < 0.001$) in retention of [8-^{14}C]-GCV in the liver, when using the AdCMV-HSV1-tk virus, as compared with the control virus for all levels of AdCMV-HSV1-tk virus tested. Even for viral titers as low as 0.50×10^9 pfu, a statistically significant difference in the net accumulation of activity in the liver was observed when results from AdCMV-HSV1-tk virus are compared with control virus. There also are statistically significant differences ($p < 0.001$) in the net accumulation of radioactivity in the liver between each viral titer (except for between 0.75×10^9 pfu and 1.0×10^9 pfu titers). The spleen also shows some [8-^{14}C]-GCV trapping that increases with increasing viral titers. The kidneys show highly variable amounts of [8-^{14}C]-GCV activity between mice, probably due to various factors (e.g., hydration status) which affect the ability of the kidneys to clear the [8-^{14}C]-GCV.

Biodistribution studies were performed in 4 mice injected with control virus at 5, 20, 90 and 120 min after injection of [8-^{14}C]-GCV. These studies revealed that there is some hepatobiliary excretion of [8-^{14}C]-GCV, with some activity in the gallbladder measured within 20 min. The [8-^{14}C]-GCV activity in the gallbladder could not be dissected separately from radioactivity in the associated liver lobe without rupturing the gallbladder. This radioactivity cleared from the gallbladder into the gastrointestinal tract by 20 min after injection, with negligible activity remaining beyond 90 min (data not shown).

In 8 of the 12 mice studied for biodistribution, liver and muscle samples were obtained for HSV1-tk mRNA and relative HSV1-TK enzyme determinations. Figure 3A shows a Northern blot using RNA extracted from the livers of 4 of the 8 mice. Shown are the results for a mouse injected with the control virus and 3 mice injected with AdCMV-HSV1-tk virus at increasing titers. Two HSV1-tk bands are observed for all mice injected with AdCMV-HSV1-tk virus, and no HSV1-tk bands are present for the mouse injected with control virus. As expected, a GAPDH band (used to normalized for RNA loading) is present for all 4 mice. The position of the bands in the lower panel is slightly variable because bands move at different rates due to local fluctuations (usually due to heating) in the gel. The correlation between the normalized HSV1-tk mRNA and the relative HSV1-TK enzyme levels from livers of the 8 mice is 0.89 (data not plotted). Shown in Figure 3B and 3C are the [8-^{14}C]-GCV %ID/g liver when using the AdCMV-HSV1-tk virus as a function of normalized HSV1-tk mRNA expression and relative HSV1-TK enzyme levels respectively for 8 mice. As the normalized HSV1-tk mRNA levels (and relative HSV1-TK enzyme levels) increase (indicating increasing levels of the HSV1-tk gene expression), there are increasing levels of [8-^{14}C]-GCV accumulation in the liver, with plateauing at higher levels of expression. The correlation coefficient for these in vivo data are 0.74 and 0.86 for HSV1-tk mRNA levels and HSV1-TK enzyme activity levels respectively (assuming a linear model). The relative levels of HSV1-TK enzyme in muscle samples are low (range: 0.2–1.0 dpm/μg protein/min) for mice injected with various levels of AdCMV-HSV1-tk. Furthermore, muscle samples from mice injected with AdCMV-HSV1-tk do not show significantly more HSV1-TK activity than muscle samples from mice injected with control virus ($p < 0.05$) (data not shown). These biodistribution data

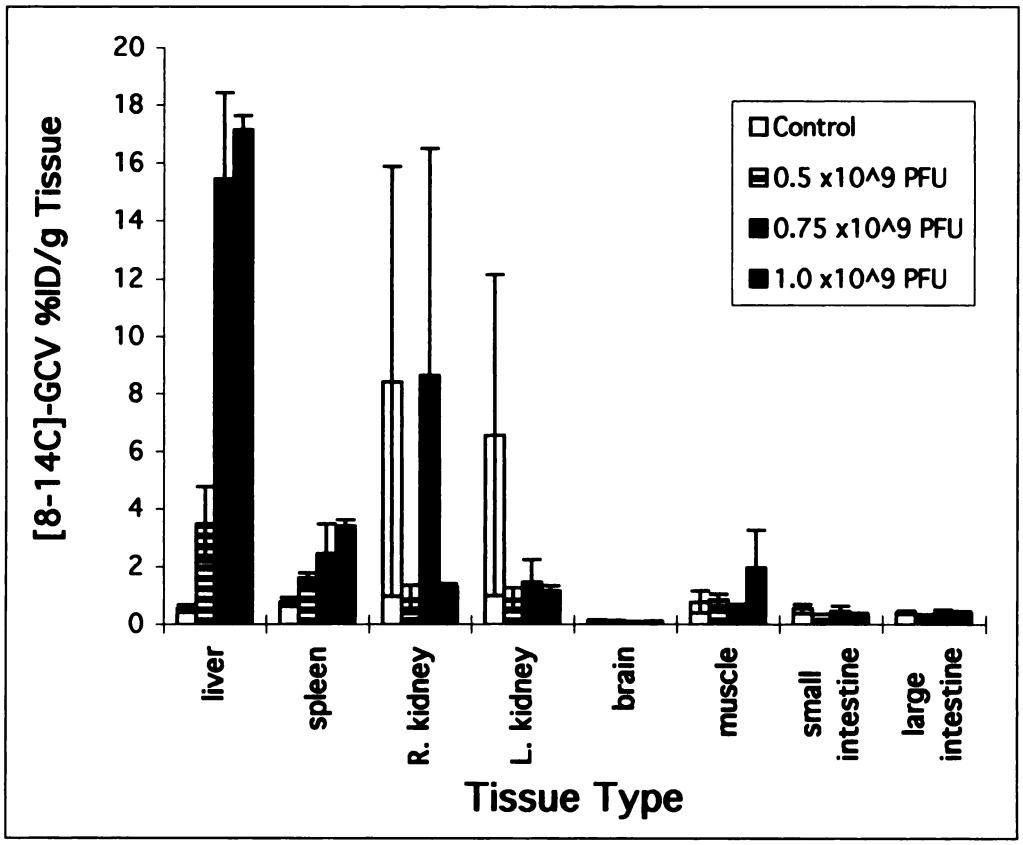

FIGURE 2. Biodistribution of [8-^{14}C]-GCV percent injected dose (%ID)/g tissue for mice injected with control virus and AdCMV-HSV1-tk virus at three different pfu levels (0.5, 0.75, 1.0 × 10^9). Each bar represents average ± s.e. for three mice.

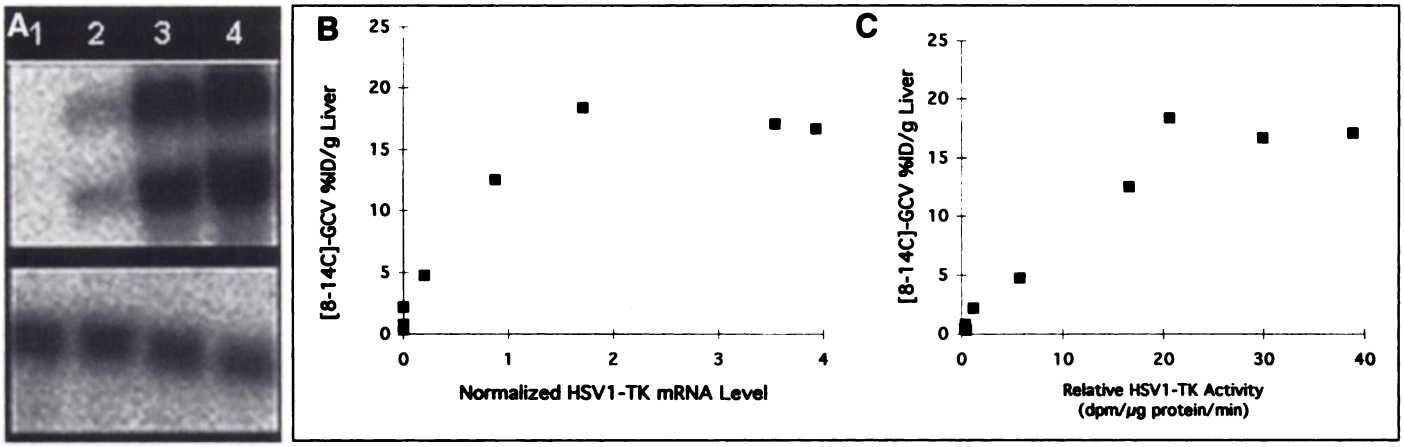

FIGURE 3. (A) Northern blot of liver samples from four mice injected with 1.0×10^9 pfu (lane 1) of control virus, or 0.5×10^9 pfu (lane 2), 0.75×10^9 pfu (lane 3), or 1.0×10^9 pfu (lane 4) of AdCMV-HSV1-tk virus. Top two bands in lanes 2–4 are from presence of HSV1-tk transcripts (upper panel) and bottom band in lanes 1–4 are from GAPDH (lower panel). (B) [8-^{14}C]-GCV %ID/g liver versus normalized HSV1-tk mRNA expression in vivo. Each of eight points represent data from different mouse injected with either control virus or AdCMV-HSV1-tk virus at three different titers. (C) [8-^{14}C]-GCV %ID/g liver versus relative HSV1-TK enzyme activity in vivo. Each of eight points represents data from different mouse injected either with control virus or AdCMV-HSV1-tk virus at three different titers as described in panel B.

supported pursuing the use of [8-^{14}C]-GCV for imaging, and therefore digital whole-body autoradiography (DWBA) was performed next.

Autoradiography

Digital whole-body autoradiography also was used to assess the utility of [8-^{14}C]-GCV as a reporter probe to image HSV1-tk reporter gene expression in vivo. Mice were injected with 0.5×10^9 pfu or 1.0×10^9 pfu of AdCMV-HSV1-tk virus or 1.0×10^9 pfu of control virus. Two days later the animals received [8-^{14}C]-GCV intravenously through a tail vein injection. One hour after [8-^{14}C]-GCV administration the animals were sacrificed for DWBA. Figure 4 shows the anatomical photographs and the 45-μM DWBA for the various animals, studied from both an anterior and a more posterior coronal section. Note the lack of signal within the liver in the mouse injected with control virus; and the relatively high levels of signal within the liver as compared to other organs in the HSV1-tk positive mice. There also is a relatively low signal obtained from most organs in both autoradiograms. Only intestinal activity and renal activity produce a relatively high level of nonspecific (not due to cells expressing HSV1-tk) signal due to the clearance of the [8-^{14}C]-GCV through these routes. Liver activity appears to be relatively homogenous within a given coronal section, but varies as much as 10%–25% across various coronal sections. Note also the lack of activity within the brain, due to the apparent inability of GCV to penetrate the blood-brain barrier and be significantly retained (*37*). The [8-^{14}C]-GCV mean % ID/g liver as measured from the DWBA from the control mouse, the mouse injected with 0.5×10^9 pfu virus, and the mouse injected with 1.0×10^9 pfu of AdCMV-HSV1-tk virus were 0.5, 3.5 and 15.4, respectively. The average ratio of %ID/g liver to %ID/g muscle was ~0.9 (control), ~3.4 (0.5×10^9 pfu AdCMV-HSV1-tk virus), and ~16.0 (1.0×10^9 pfu AdCMV-HSV1-tk virus) in these autoradiograms (depending on the exact location of the regions of interest). These data demonstrate both a high imaging sensitivity and specificity for imaging the expression of the HSV1-tk reporter gene, using [8-^{14}C]-GCV as a reporter probe. The data also demonstrate a good target-to-background ratio. Three additional murine DWBA studies produced similar imaging results (data not shown).

microPET Imaging

To *preliminarily* test the feasibility of imaging HSV1-tk reporter gene expression with [8-^{18}F]-FGCV and microPET, we next performed studies with a murine model using the adenoviral vector delivery system. Shown in Figure 5 is a coronal section from the microPET scan of one mouse injected with control virus and one mouse injected with AdCMV-HSV1-tk virus. Clear localization of radioactivity to the liver is seen in the mouse injected with AdCMV-HSV1-tk virus as compared to the mouse injected with control virus. Bladder and intestinal activity is also seen in both images. After sacrificing the animal, the %ID/g liver (left lobe) ± s.e. was determined by well counting (corrected for efficiency) to be 0.32% ± 0.24 and 1.8% ± 0.9 in the 3 mice injected with control virus and 3 injected with AdCMV-HSV1-tk virus, respectively ($p < 0.01$). Furthermore, [8-^{18}F]-FGCV is stable in mouse serum with > 98% excreted unchanged in the urine in 60 min.

DISCUSSION

The C6 cell culture data support the hypothesis that the net accumulation of [8-^{3}H]-GCV in cells is directly attributable to successful adenoviral delivery of the HSV1-tk gene. Also, for C6 cells not expressing the HSV1-tk gene (those exposed to control virus), there is significantly less net accumulation of [8-^{3}H]-GCV. Furthermore, the cell culture data demonstrate the relatively low sensitivity of [side-chain−2-^{3}H]-ACV, because of a lack of sufficient accumulation of this tracer in reasonably short times. The cell culture results support the investigation of [8-^{14}C]-GCV (which produces better DWBA results as compared to those with [8-^{3}H]-GCV) for biodistribution and DWBA studies.

Biodistribution results by direct tissue analysis show that hepatic [8-^{14}C]-GCV can accumulate in sufficient amounts in relatively short time periods to image the expression of successful HSV1-tk reporter gene transduction in vivo. High correlations in vivo between HSV1-tk mRNA levels, relative HSV1-TK enzyme activity levels, and the [8-^{14}C]-GCV %ID/g tissue (good sensitivity) were shown. We observe a possible plateauing of the [8-^{14}C]-GCV %ID/g liver as the normalized HSV1-tk mRNA levels and the relative HSV1-TK enzyme levels increase. Additional data will be needed to further study this plateauing effect and to determine if it is significant, or if in fact a strictly linear relationship exists. If a plateauing effect

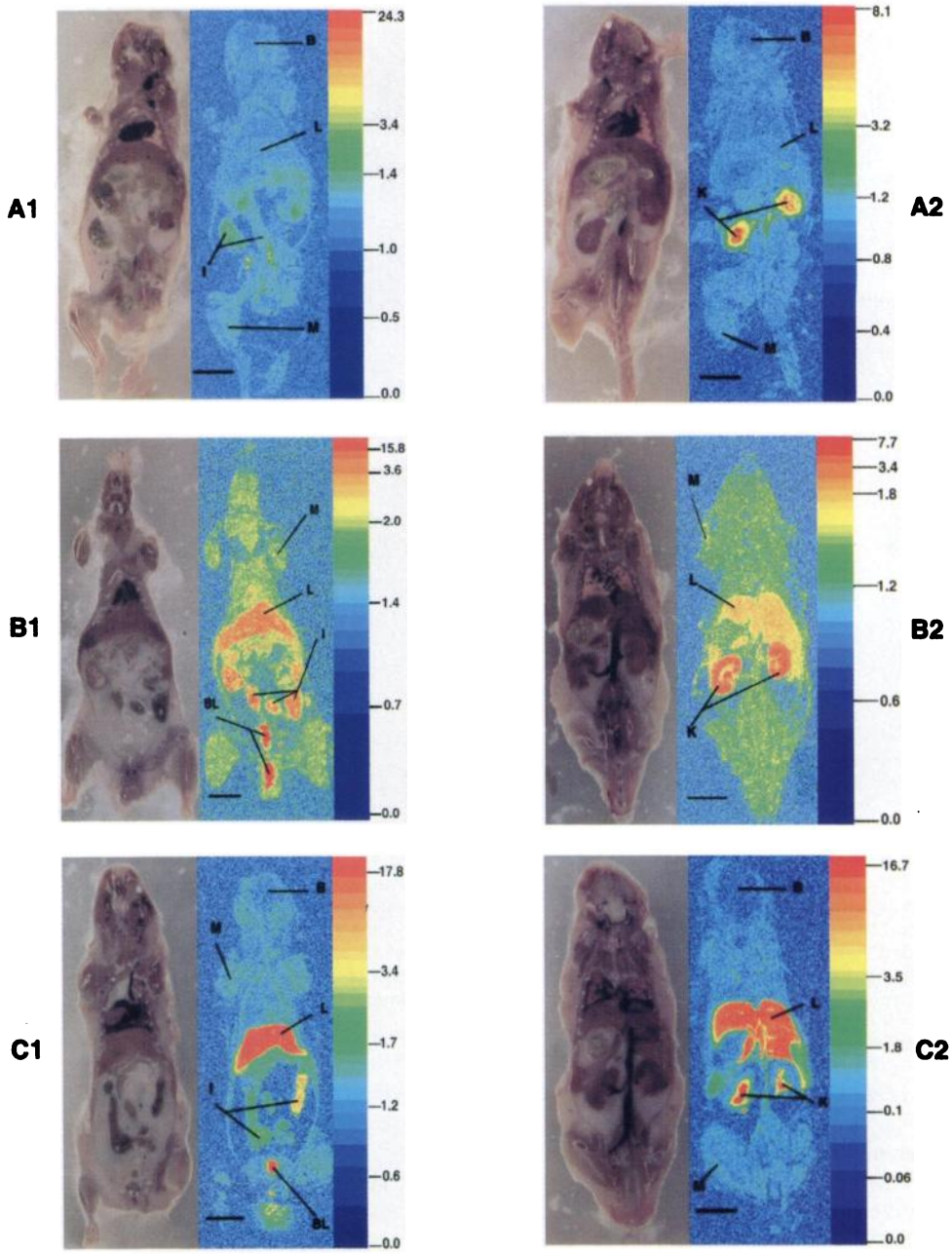

FIGURE 4. (A, B, C) DWBA from three mice. (A1, B1, C1) anterior and (A2, B2, C2) posterior coronal cross-sections. Images A1, A2 are for mouse injected with 1.0×10^9 pfu of control virus. Images B1, B2 and C1, C2 are for mice injected with 0.5×10^9 and 1.0×10^9 pfu of AdCMV-HSV1-tk virus, respectively. In each case mouse anatomical coronal cross-section photograph (left-side) and corresponding DWBA (right-side) are shown. Each mouse was injected with virus ~48 hr before injection of [8-^{14}C]-GCV. Each mouse was sacrificed ~60 min after injection of [8-^{14}C]-GCV. Horizontal scale bar = 10 mm. DWBA pixels represent the % ID/g tissue as shown in each intensity scale to right of DWBA. Note that each scale is nonlinear and different for each DWBA to enhance outline of mouse relative to various signals seen within given coronal cross-section. L = liver; K = kidney; I = intestine; M = muscle; B = brain; BL = bladder.

holds in studies with more animals, then the %ID/g liver may underestimate the total level of gene expression for higher levels of expression. A high level of specificity is observed, with relatively low %ID/g from nontransduced tissues, when animals are injected with [8-^{14}C]-GCV. Elimination of the tracer primarily by the kidneys and minimally by the hepatobiliary system was also shown. Based on these results, DWBA was used to evaluate [8-^{14}C]-GCV as an imaging probe.

The DWBA results further support the sensitivity and specificity results obtained from the biodistribution studies. A good contrast between the radioactivity signal from liver and background is obtained. Moreover, this contrast decreases when lower viral titers of AdCMV-HSV1-tk were administered. These results therefore suggest that the HSV1-tk reporter gene and a suitable positron-labeled ganciclovir reporter probe system should be useful for noninvasively and quantitatively imaging reporter gene expression with PET, and warrant the investigation of a PET based approach. These data are the first to show the feasibility of a ganciclovir based approach for imaging HSV1-tk reporter gene expression in vivo. Although ganciclovir has been previously studied in cell culture (*6,10*), it is important to validate its utility in vivo before the study of labeled ganciclovir for use with PET imaging.

In vivo murine studies were performed with an adenoviral delivery mechanism, as opposed to performing studies in tumor cell lines. The viral approach permits easy modification of HSV1-tk expression by changing adenoviral dose, and a quick experiment turnover time since tumors need not be grown. This model also allows for a relatively homogeneous level of HSV1-tk expression, an experimental parameter that is not easily possible with a tumor model. The adenoviral model used in this study is useful because gene delivery is restricted primarily to the liver. Low levels of HSV1-tk delivery and expression to non-liver tissues do occur, but do not effect the results of this study significantly. The control tissue (muscle) studied showed only relatively low levels of HSV1-TK, and other tissues are also expected to be low as has been reported previously in other adenoviral models (*26*). Studies to compare

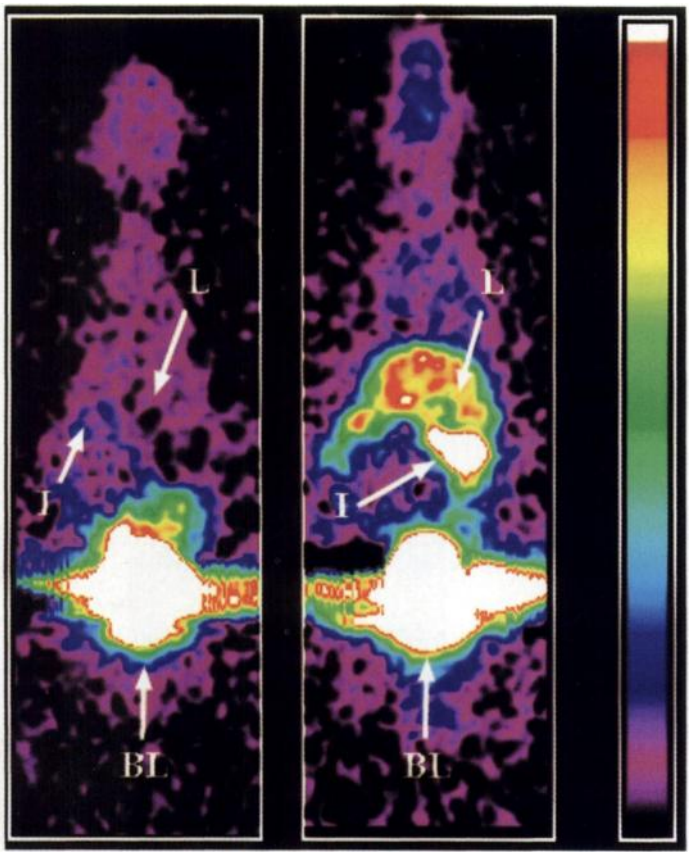

FIGURE 5. [8-^{18}F]-FGCV coronal microPET images from mouse injected with control virus (left) and AdCMV-HSV1-tk virus (right). Each viral vector was injected 48 hr before injection of [8-^{18}F]-FGCV. MicroPET images were obtained 1 hr after injection of [8-^{18}F]-FGCV using eight bed positions and 8 min/bed. Each image is normalized to common global maximum with thresholding and represents ~1-mm depth and in-plane resolution of ~3 mm. Color scale is as indicated, with white representing maximum counts. L = liver; I = intestine; BL = bladder.

results of reporter probe net accumulation from tumor cells expressing HSV1-tk, grown in cell culture and in vivo in a nude mouse model are currently under way, and will be reported elsewhere.

Several probes including acyclovir, ganciclovir, FIAU and derivatives of FIAU have been discussed as potential positron-labeled substrates for imaging HSV1-tk gene expression by PET (*3–5*). The factors to be considered in evaluating these alternative substrates as PET reporter probes to image HSV1-tk reporter gene expression include: (a) the half-life of the radionuclide relative to the pharmacokinetics of the probe; (b) the percents of decay that lead to positron emission for a given radionuclide; (c) the ease of production and availability of the radionuclide and probe; (d) the in vivo stability of the labeled substrate; (e) the relative affinity of the tracer for HSV1-TK and mammalian thymidine kinases; and (f) the pharmacokinetics and route(s) of clearance of the tracer.

Tjuvajev et al. (*6*) explored the utility of ganciclovir and FIAU in cell culture studies. Our study shows for the first time the utility of labeled ganciclovir as a probe for imaging gene expression in vivo. Although FIAU has a greater affinity for HSV1-tk than does ganciclovir, FIAU also has a significant affinity for mammalian thymidine kinases leading to a greater background signal (*6,7*). Therefore, one may have to wait longer for washout of background activity (*6,7*) before imaging. However, if there is sufficiently high HSV1-tk expression in target tissue, then the amount of time needed for washout of FIAU may be able to be reduced. Further direct comparisons between various labeled forms of FIAU and ganciclovir in vivo are currently under way in our laboratory.

The true sensitivity and specificity for any probe in vivo depends in part on the route(s) of elimination of the probe. In the case of [8-^{14}C]-GCV, the primary route of elimination is through the kidneys. However, it was observed that [8-^{14}C]-GCV also is eliminated by the hepatobiliary system. There is a purine salvage pathway associated with the hepatobiliary system (*38*), which is consistent with the observed hepatobiliary excretion of tracer. Therefore, for HSV1-tk reporter gene expression relatively near the kidneys, urinary bladder, gallbladder and/or gastrointestinal tract, appropriate timing of imaging will help improve the overall sensitivity and specificity of the assay. The lower limit of detectability of HSV1-TK levels while using labeled ganciclovir has not been characterized in the present work, although injection of 0.50×10^9 pfu of AdCMV-HSV1-tk leads to detectable trapped [8-^{14}C]-GCV. The percent of hepatocytes infected using 0.50×10^9 pfu and 1.0×10^9 pfu is 2% ± 2% and 9% ± 2%, respectively (unpublished data determined by using a β-galactosidase expressing virus). The lowest level of detectability in vivo is a complex issue, which will depend on the exact activity in regions surrounding transduced tissue as well as the competing level of intracellular thymidine. The current study has not attempted to separate the transport from phosphorylation of tracer. It is possible that different tissues may express different levels of transporters for ganciclovir, which would complicate interpretation of the results. Future kinetic studies should be helpful in determining if transport is rate limiting in any way, and may help to kinetically distinguish ganciclovir transport from HSV1-tk dependent phosporylation.

We have only preliminarily studied [8-^{18}F]-FGCV as a reporter probe for HSV1-tk imaging in vivo, to demonstrate that this tracer is worth pursuing in greater detail. Cell culture studies, arterial input function characterization, peripheral metabolism of this probe, correlations with PET signal and relative HSV1-tk gene expression, optimal timing to allow background intestinal activity to clear, and the relative quantitation of gene expression by [8-^{18}F]-FGCV (through a tracer kinetic model) are currently under way and will be reported elsewhere. These investigations, along with enzyme kinetic data will help to further define the potential role of [8-^{18}F]-FGCV and PET for imaging HSV1-tk reporter gene expression.

The most immediate practical application of PET-imaged reporter gene expression will be for human gene therapy (*39*). In one gene therapy approach, cultured cells are transfected with a therapeutic gene and then transferred to the patient. In this adoptive-cell gene therapy paradigm, it is difficult to determine if the transplanted cells reach their target site, how long the transplanted cells remain viable, and whether or not expression of the therapeutic gene is subsequently compromised. In a second gene therapy approach, DNA packaging and delivery systems (e.g., viruses, liposomes) containing therapeutic genes are introduced directly into the patient; the packaging system is intended to target the therapeutic gene to the appropriate cells. After administration of the reporter gene, the physician has no means of monitoring localization or expression of the therapeutic gene. Appropriate PET reporter genes, administered in conjunction with the therapeutic gene(s), will permit physicians to use PET reporter probes and tomographic analysis to repeatedly monitor the localization, proliferation, and function both of cells used in adoptive-cell gene therapy and of DNA delivery systems administered directly to patients. In addition to use for human gene therapy, the HSV1-tk/[8-^{18}F]-FGCV system should be usable in various animal studies

for studying the expression and regulation of various genes. Using PET reporter probes in transgenic animals, in which the regulatory region of the gene of interest drives a transcript encoding a PET reporter gene, it will be possible to repeatedly monitor, in the same animal, time-dependent developmental, environmental and experimental influences on gene expression.

CONCLUSION

This study demonstrates the feasibility of using [8-^{14}C]-ganciclovir as a reporter probe for the HSV1-tk reporter gene, using an in vivo adenoviral-mediated gene delivery system in a murine model. Successful imaging of reporter gene expression in murine liver was demonstrated using digital whole-body autoradiography and the liver signal was related directly to the level of gene expression. High specificity and sensitivity were demonstrated. Preliminary results using [8-^{18}F]-FGCV support a PET-based assay for imaging reporter gene expression.

ACKNOWLEDGMENTS

We thank Drs. Margaret E. Black (Chiroscience R&D, Inc., Bothell, WA) and Srinivasta Reddy for helpful discussions. We thank Ron Sumida, Judy Edwards, Alan Oshiro, Waldemar Ladno, Parag Shah, Matthew Allen and Vaughn Davis for technical assistance and Diane Martin and Theresa Sama for their help in preparing this manuscript. This work was partially supported by funding from DOE contract DE-FC03-87ER60615, the University of California Biotechnology Grant, the Dana Foundation and the UCLA-Jonsson Comprehensive Cancer Center. Lily Wu was supported by a HHMI physician postdoctoral fellowship.

REFERENCES

1. Chalfie M, Tu Y, Euskirchen W, Ward W, Prasher DC. Green fluorescent protein as a marker for gene expression. *Science* 1994;263:802–805.
2. Jacobs WR, Barletta RG, Udani R, et al. Rapid assessment of drug susceptibilities of *Mycobacterium tuberculosis* by means of luciferase reporter phages. *Science* 1993; 260:819–822.
3. Morin KW, Atrazheva ED, Knaus EE, Wiebe LI. Synthesis and cellular uptake of 2'-substituted analogues of (E)-5-(2-[125I]Iodovinyl)-2'-deoxyuridine in tumor cells transduced with the herpes simplex type-1 thymidine kinase gene. Evaluation as probes for monitoring gene therapy. *J Med Chem* 1997;40:2184–2190.
4. De Clercq E. Biochemical aspects of the selective antiherpes activity of nucleoside analogues. *Biochem Pharmacol* 1984;33:2159–2169.
5. Watanabe K, Reichman U, Hirota K, Lopez C, Fox J. Nucleosides synthesis and anitherpes virus activity of some 2'-fluoro-2'deoxy-arabinofuranosyl-pyrimidine nucleosides. *J Med Chem* 1979;22:21–24.
6. Tjuvajev JG, Stockhammer G, Desai R, et al. Imaging the expression of transfected genes in vivo. *Cancer Res* 1995;55:6126–6132.
7. Tjuvajev JG, Finn R, Watanabe K, et al. Noninvasive imaging of herpes virus thymidine kinase gene transfer and expression: a potential method for monitoring clinical gene therapy. *Cancer Res* 1996;56:4087–4096.
8. Tjuvajev J, Avrill N, Safer M, et al. Quantitative PET imaging of HSV1-TK gene expression with [I-124]FIAU [Abstract]. *J Nucl Med* 1997;38:239P.
9. Srinivasan A, Gambhir SS, Green LA, et al. A PET reporter gene (PRG)/PET reporter probe (PRP) technology for repeatedly imaging gene expression in living animals [Abstract]. *J Nucl Med* 1996;37:107P.
10. Haberkorn U, Altmann A, Morr I, et al. Monitoring gene therapy with herpes simplex virus thymidine kinase in hepatoma cells: uptake of specific substrates. *J Nucl Med* 1997;38:287–294.
11. Haberkorn U, Oberdorfer F, Gebert J, et al. Monitoring of gene therapy with cytosine deaminase: in vitro studies using 3H-5-fluorocytosine. *J Nucl Med* 1996;37:87–94.
12. Herschman HR, Sharfstein S, Gambhir SS, et al. In vivo imaging of gene expression associated with cell replication [Abstract]. *J Nucl Med* 1997;38:250P.
13. O'Brien JJ, Campoli-Richards DM. Acyclovir. An updated review of its antiviral activity, pharmacokinetic properties and therapeutic efficacy. *Drugs* 1989;37:233–309.
14. Faulds D, Heel RC. Ganciclovir. A review of its antiviral activity, pharmacokinetic properties and therapeutic efficacy in cytomegalovirus infections. *Drugs* 1990;39:597–638.
15. Mahony WB, Domin BA, McConnell RT, Zimmerman TP. Acyclovir transport into human erythrocytes. *J Biol Chem* 1988;263:9285–9291.
16. Mahony WB, Domin BA, Zimmerman TP. Ganciclovir permeation of the human erythrocyte membrane. *Biochem Pharm* 1991;41:263–271.
17. Elion GB. Mechanism of action and selectivity of acyclovir. *Am J Med* 1982;73:7–13.
18. Balzarini J, Bohman C, De Clercq E. Differential mechanism of cytostatic effect of (E)-5-(2-bromovinyl)-2'-deoxyuridine, 9-(1,3-dihydroxy-2-propoxymethyl) guanine, and other antiherpetic drugs on tumor cells transfected by the thymidine kinase gene of herpes simplex virus type 1 or type 2. *J Biol Chem* 1993;268:6332–6337.
19. de Miranda P, Krasny HC, Page DA, Elion GB. The disposition of acyclovir in different species. *J Pharmacol Exp Ther* 1981;219:309–315.
20. Barrio JR, Namavari M, Phelps ME, Satyamurthy N. Regioselective fluorination of substituted guanines with dilute F2: a facile entry to 8-fluoroguanine derivatives. *J Org Chem* 1996;61:6084–6085.
21. Barrio JR, Namavari M, Phelps ME, Satymamurthy N. Elemental fluorine to 8-fluoropurines in one step. *J Am Chem Soc* 1996;118:10408–10411.
22. Barrio JR, Namavari M, Srinivasan A, et al. Carbon-8 radiofluorination of purines: a general approach to probe design for gene therapy in humans. *XIIth International Symposium on Radiopharmaceutical Chemistry* 1997:348.
23. Monclus M, Luxen A, Cool V, Damhaut P, Velu T, Goldman S. Development of a positron emission tomography radiopharmaceutical for imaging thymidine kinase gene expression: synthesis and in vitro evaluation of 9-{(3-[F-18]fluoro-1-hydroxy-2-propoxy)methyl}guanine. *Bioorg Med Chem Lett* 1997;7:1879–1882.
24. Alauddin MM, Conti PS, Mazza SM, Hamzeh FM, Lever JR. 9-[(3-[^{18}F]-fluoro-1-hydroxy-2-propoxy)methyl]guanine ([18F]-FHPG): a potential imaging agent of viral infection and gene therapy using PET. *Nuc Med Biol* 1996;23:787–792.
25. Bading JR, Alauddin MM, Fissekis JH, Kirkman E, Raman RK, Conti PS. Pharmacokinetics of F-18 fluorohydroxypropoxymethylguanine (FHPG) in primates [Abstract]. *J Nucl Med* 1997;38:43P.
26. Herz J Girard RD. Adenovirus-mediated transfer of low density lipoprotein receptor gene acutely accelerates cholesterol clearance in normal mice. *Proc Nat Acad Sci USA* 1993;90:2812–2816.
27. Cherry SR, Shao Y, Silverman RW, et al. microPET: a high resolution PET scanner for imaging small animals. *IEEE Transactions on Nucl Sci* 1997;44:1161–1166.
28. Smith GN, Ludwig DP, Wright KC, Bauriedel WR. Simple apparatus for combustion of samples containing C14-labeled pesticides for residue analysis. *Agricul Food Chem* 1964;12:172–175.
29. Gomez-Foix AM, Coats WS, Baques S, Alam T, Girard RD, Newgard CB. Adenovirus-mediated transfer of the muscle glycogen phosphorylase gene into hepatocytes confers altered regulation of glycogen metabolism. *J Biol Chem* 1992;267:25129–134.
30. Jones N, Shenk T. Isolation of adenovirus type 5 host range deletion mutants defective for transformation of rat embryo cells. *Cell* 1979;17:683–689.
31. Grodzicker T, Klessig DF. Expression of unselected adenovirus genes in human cells co-transformed with the HSV-1tk gene and adenovirus 2 DNA. *Cell* 1980;21:453–463.
32. Bradford MM. A Rapid and sensitive method for the quantitation of microgram quantities of protein utilizing the principle of proteint-dye binding. *Anal Biochem* 1976;72:248–254.
33. Hruby DE, Ball AL. Cell-free synthesis of enzymatically active vaccinia virus thymidine kinase. *Virology* 1981;113:594–601.
34. Chomczynski P, Mackey K. Modification of the TRI Reagent™ procedure for isolation of RNA from polysaccharide- and proteoglycan-rich sources. *BioTechniques* 1995;19:942–945.
35. Kawamoto T, Shimizu M. A method for preparing whole-body sections suitable for autoradiographic, histological, and histochemical studies. *Stain Technol* 1986;61:169–183.
36. Lear JL. Principles of single and multiple radionuclide autoradiography, Chapter 5. In: *Positron emission tomography and autoradiography: principles and applications for the brain and heart.* New York: Raven Press; 1986:197–235.
37. Brewster ME, Raghavan K, Pop E, Bodor N. Enhanced delivery of ganciclovir to the brain through the use of redox targeting. *Antimicrobial Agents and Chemotherapy* 1994;38:817–823.
38. Che M, Gatmaitan Z, Arias IM. Ectonucleotidases, purine nucleoside transporter, and function of the bile canalicular plasma membrane of the hepatocyte. *FASEB J* 1997;11:101–108.
39. Moolten FL. Suicide genes for cancer therapy. *Science and Medicine* 1997;4:16–25.